

Near edge x-ray absorption fine structure spectroscopy with x-ray free-electron lasers

D. P. Bernstein,^{1,a)} Y. Acremann,¹ A. Scherz,¹ M. Burkhardt,¹ J. Stöhr,¹ M. Beye,² W. F. Schlotter,² T. Beeck,² F. Sorgenfrei,² A. Pietzsch,² W. Wurth,² and A. Föhlisch²
¹SLAC National Accelerator Laboratory, 2575 Sand Hill Road, Menlo Park, California 94025, USA
²Institut für Experimentalphysik and Centre for Free-Electron Laser Science, Universität Hamburg, Luruper Chaussee 149, 22761 Hamburg, Germany

(Received 21 May 2009; accepted 12 August 2009; published online 28 September 2009)

We demonstrate the feasibility of near edge x-ray absorption fine structure spectroscopy on solids by means of femtosecond soft x-ray pulses from a free-electron laser (FEL). Our experiments, carried out at the FEL at Hamburg used a special sample geometry, spectrographic energy dispersion, single shot position-sensitive detection, and a data normalization procedure that eliminates the severe fluctuations of the incident intensity in space and photon energy. As an example, we recorded the $^3D_1 N_{4,5}$ edge absorption resonance of La^{3+} ions in LaMnO_3 . Our study opens the door for x-ray absorption measurements on future x-ray FEL facilities. © 2009 American Institute of Physics. [doi:10.1063/1.3236540]

Near edge x-ray absorption fine structure (NEXAFS) experiments are based on the ability to fine-tune the incident photon energy across core electron excitation thresholds with sub-eV resolution and step size. While at conventional synchrotron radiation sources energy selection and tuning are accomplished by a monochromator, the intrinsic spectrum of an x-ray free-electron laser (FEL) is ill suited for such measurements.^{1,2} Based on the self-amplified spontaneous emission (SASE) process of FELs, the photon spectrum is peaked at an energy E that stochastically fluctuates shot-to-shot by an amount comparable to the energy width ΔE of each single pulse. Hence, if a monochromator is used to control the excitation energy, the intensity greatly fluctuates and may even be zero for certain pulses. This leads to severe intensity normalization problems. The variation in shot-to-shot emitted spectral peak position and width ($\Delta E/E \approx 3 \times 10^{-3}$)³ is much smaller than the typical range of a NEXAFS spectrum (>10 eV) so that tuning of the photon energy E is required. For the first generation of x-ray FELs equipped with fixed gap undulators, this can only be accomplished via fine tuning of the electron beam energy. Because of the unusual characteristics of the emitted FEL radiation, x-ray absorption spectroscopy has been largely deemed difficult with such sources.

The NEXAFS technique is commonly used at synchrotron sources to investigate bonding at surfaces, in thin films, and in liquids.⁴⁻⁶ By sum rule analysis of polarization dependent spectral peak intensities, it allows the decoupling of charge, orbital moment, and spin moment contributions to the electronic structure in complex materials.^{7,8} NEXAFS is also closely related to modern x-ray imaging techniques which, with the advent of x-ray FELs, will become important in the study of femtosecond dynamics governing atomic motion and the processes underlying energy and angular momentum transfer between electronic, spin, and lattice degrees of freedom.^{7,9-11} The measurement of the intensity of NEXAFS resonances as a function of incident flux of x-ray FELs will be important in understanding photon-sample interac-

tions. In particular, it will be essential to understand the conditions under which an x-ray FEL pulse can no longer be treated as a weak perturbation of the electronic structure, i.e., the intensity under which the x-ray perturbation will lead to radically altered electronic states and enter the realm of nonlinear and multiphoton processes as well as field-induced modifications.¹²⁻¹⁴

The purpose of this work is to show the feasibility of NEXAFS on a solid sample using the soft x-ray radiation generated by the Free-electron Laser at Hamburg (FLASH). The statistical intensity, photon energy, and mode distribution of the femtosecond x-ray pulses generated in single pass SASE mode required the development of a suitable experimental method. The experiment was performed at the PG2 monochromator beamline at FLASH,¹⁵ which was operated at 5 Hz repetition rate. The experimental setup is shown in Fig. 1.

Radiation from the FLASH beam is dispersed in energy in the vertical direction by grating before illuminating the sample. The sample consists of a lithographically fabricated

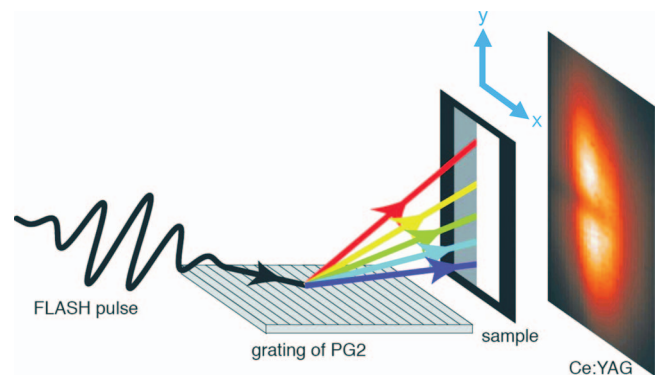


FIG. 1. (Color) Cartoon of NEXAFS in single shot spectrograph detection at FLASH. Femtosecond x-ray pulses from the SASE undulator disperse on the monochromator grating and pass through the sample. The sample is two-parted for simultaneous measurement of the absorption in the thin-film sample and the unmodified reference spectral distribution for single shot normalization. The transmitted x-rays are converted into visible light on a Ce:YAG crystal and imaged with an ICCD.

^{a)}Electronic mail: dpb167@stanford.edu.

100 nm thick Si_3N_4 membrane window with a vertical dimension of 12 mm and a horizontal dimension of 2 mm. At the sample position, the beam is dispersed by 0.3 eV/mm leading to an energy range of approximately 4 eV. The membrane is divided horizontally with 75 nm of LaMnO_3 deposited on half of the membrane by pulsed laser deposition and the use of a shadow mask.¹⁰ The other half of the nitride window is left blank. This is a critical feature of the sample as it allows us to capture information such as incident intensity and energy spectrum on a shot-by-shot basis. Absorption is measured via transmission onto a Ce:yttrium aluminum garnet (YAG) crystal placed behind the sample. The fluorescent light from the Ce:YAG crystal is imaged by an intensified charge coupled device camera (ICCD). The vertical y -axis on the detector records the spectral information of the sample.

We chose LaMnO_3 for this experiment because the $N_{4,5}$ edge of the La^{3+} ions in LaMnO_3 exhibits an atomically sharp 3D_1 absorption resonance at a photon energy of 102.17 eV, where the Si_3N_4 membrane is highly transparent. The homogeneity of the deposited film is essential for our spectroscopy scheme. The sample was placed 5 cm away from the target during the pulsed laser deposition in order to optimize uniformity. The energetic position and the narrow spectral width of the 3D_1 absorption resonance is due to the localization of the La $4f$ states. The central FLASH photon energy was varied over a range of approximately 2 eV by changing the energy of the electron beam in order to collect statistics uniformly across the energy range of interest.

In a first step, we calibrated our detection scheme, consisting of the Ce:YAG fluorescence converting crystal and the ICCD with respect to detection response. Since the incident intensity varies between pulses and within images, it is essential to correct for these nonlinearities in the detection scheme. We recorded 2000 pulses with no sample in the beam. To compensate the nonlinear response of the detector we use the ansatz $I[f(x,y)] = a_1f + a_2f^2 + a_3f^3 + a_4f^4$, where I is the true intensity on a particular pixel, $f(x,y)$ is the detector signal on that pixel, a_1 characterizes the linear sensitivity of the detector, and $a_2 \dots a_4$ characterize the nonlinear saturation. The total pulse intensity $I_{\text{tot, gm}}$ is measured simultaneously by a gas monitor detector placed in the FEL beamline before the grating. The monochromator was operated using a 200 l/mm grating yielding an efficiency of $28.7 \pm 1\%$ for 97.8 eV radiation.¹⁶ From the detector signal $f(x,y)$, $I(f)$ gives the x-ray intensity per pixel. By comparing the total pulse intensity measured by the gas monitor detector $I_{\text{tot, gm}}$ with the total intensity reconstructed from the detector signal $I_{\text{tot, d}} = \sum_{x,y} I(x,y)$, a square error can be constructed: $\epsilon = \sum_i (I_{\text{tot, gm}, i} - I_{\text{tot, d}, i})^2$ where the sum acts over the individual FEL pulses. The square error ϵ is minimized iteratively as a function of the parameters $a_1 \dots a_4$. The results of the correction are shown in Fig. 2. The values of the parameters $a_1 \dots a_4$ were calculated to be the following: $a_1 = 0.0655$, $a_2 = 0.04481$, $a_3 = -1.5068$, and $a_4 = 14.86$.

The illumination of the sample along the horizontal (nondispersive) x -direction fluctuates on a pulse-by-pulse basis. The mode profile along the x direction must be taken into account on a pulse-by-pulse basis in order to normalize the spectra correctly. The sum along y for each x position determines the mode profile $I_m(x) = \sum_y I(x,y)$. A reference spectrum without sample can be determined as $S_x(y)$

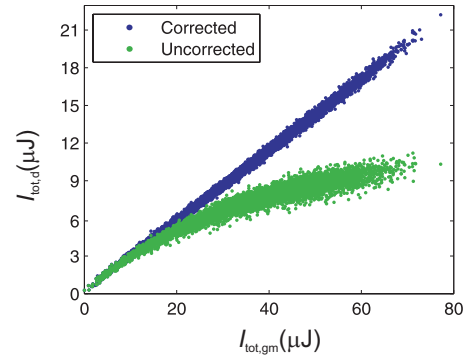


FIG. 2. (Color) Linearization of the detector: The integrated photon energy on the detector for 2000 pulses is shown as a function of the photon energy measured by the gas monitor detector of FLASH. The green dots show the raw detector data whereas the blue curve shows the data after correction for nonlinearities.

$= \langle I(x,y)/I_m(y) \rangle_x$ where $\langle \dots \rangle_x$ indicates the average along the x -direction. Dividing the columns by I_m compensates for inhomogeneities due to the mode shape and fluctuations of the beam position along x . Similarly, the pixels on the sample side are normalized by the mode profile and normalized by the reference spectrum. The normalization by the reference spectrum causes the spectrum to be insensitive to fluctuations of the photon energy distribution. This way, a normalized NEXAFS spectrum can be obtained, which is insensitive to the fluctuations of the FEL beam. The spectra resulting from single pulses are then averaged in order to obtain the spectrum shown in Fig. 4. The energy fluctuations ($\Delta E/E \approx 3 \times 10^{-3}$ shot-to-shot, $\Delta E/E \approx 0.01$ overall), in fact, help to probe a larger energy range. Notice that the monochromator focuses the beam onto the sample in the y -direction. Therefore, our detection scheme is also insensitive to the mode profile along the y -direction. Figure 3 shows two different detected x-ray pulses as well as the average over all pulses detected during the experiment.

It is essential to keep track of cumulative errors involving the individual data processing steps, starting with the statistical error $\epsilon = 1/\sqrt{I}$. In order to reduce the weight of “dark” pixels, which contain large errors, in the averages and to avoid excessive noise from divisions by small numbers, the averages were weighed by $1/\epsilon^2$. The normalized average of all pixels with a pulse energy density above 0.2 mJ/cm^2

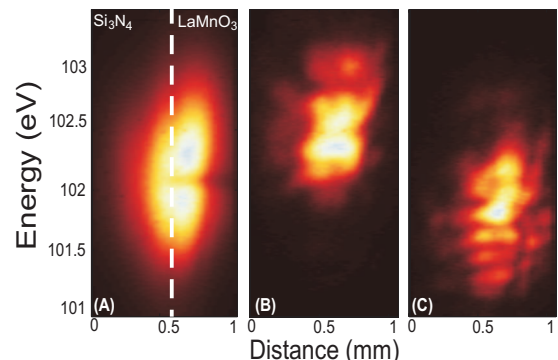


FIG. 3. (Color) (a) Sum over all the pulses of the experiment with the sample in the beam. The La absorption peak is visible at 102.17 eV. (b) and (c) Examples of FLASH pulses with no sample in the beamline. The energy, as well as mode profile, fluctuates on a pulse by pulse basis, requiring the detection of a reference spectrum for each pulse.

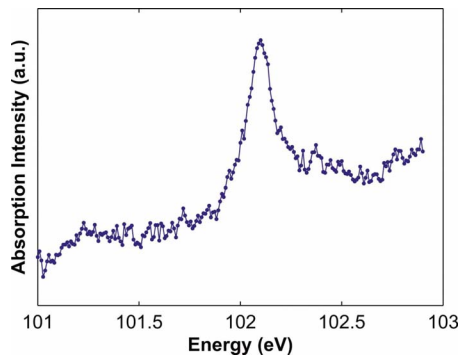


FIG. 4. (Color online) The 3D_1 absorption resonance at the $N_{4,5}$ edge of the La^{3+} ions in LaMnO_3 from all accumulated FLASH pulses.

(the highest detected pulse energy density on any pixel is $2 \text{ mJ}/\text{cm}^2$) leads to the spectrum shown in Fig. 4. It clearly exhibits the ${}^3D_1 N_{4,5}$ edge absorption resonance of La^{3+} ions in LaMnO_3 , demonstrating the feasibility of NEXAFS spectroscopy using FEL radiation.

In conclusion, we have demonstrated the feasibility of NEXAFS spectroscopy on solids using femtosecond soft x-ray pulses from the single pass SASE FEL at FLASH. Challenges presented by shot-to-shot beam fluctuations in intensity, energy, and position were overcome by a suitable experimental geometry and a numerical normalization procedure. Our study was restricted to a small energy range covering a narrow absorption resonance, typical for transition and rare earth ions, but the method can readily be extended to larger spectral windows and to higher photon energies, where the most important absorption edges are found. Future experiments at facilities such as LCLS will be able to illuminate the sample before the pulse is incident on the monochromator. This will allow for investigations at higher fluence and time resolution as monochromator efficiency and pulse stretching limit these two quantities, respectively.

The authors gratefully acknowledge the staff of the FLASH facility, in particular N. Guerassimova and R.

Treusch. This work was supported by the German Ministry of Education and Research (BMBF) through the priority program FSP301-FLASH and by the U.S. Department of Energy, Office of BES. Samples were prepared at the Stanford SNF and the laboratory of A. Kapitulnik.

- ¹A. Kondratenko and E. L. Saldin, *Part. Accel.* **10**, 207 (1980).
- ²R. Bonifacio, C. Pellegrini, and L. M. Narducci, *Opt. Commun.* **50**, 373 (1984).
- ³W. Ackermann *et al.*, *Nat. Photonics* **1**, 336 (2007).
- ⁴J. Stöhr, *NEXAFS Spectroscopy* (Springer, Berlin, 1992).
- ⁵P. Zeppenfeld, in *Physics of Covered Solid Surfaces. I. Adsorbed Layers on Surfaces*, edited by H. P. Bonzel and W. Martinsson (Springer, Berlin, 2005), Vol. 42.
- ⁶P. Wernet, D. Nordlund, U. Bergmann, M. Cavalleri, M. Odelius, H. Ogasawara, L. A. Näslund, T. K. Hirsch, L. Ojamäe, P. Glatzel, L. G. M. Pettersson, and A. Nilsson, *Science* **304**, 995 (2004).
- ⁷J. Stöhr and H. C. Siegmann, *Magnetism: From Fundamentals to Nano-scale Dynamics* (Springer, Berlin, 2006).
- ⁸D. J. Huang, W. B. Wu, G. Y. Guo, H.-J. Lin, T. Y. Hou, C. F. Chang, C. T. Chen, A. Fujimori, T. Kimura, H. B. Huang, A. Tanaka, and T. Jo, *Phys. Rev. Lett.* **92**, 087202 (2004).
- ⁹A. Cavalleri, M. Rini, H. H. W. Chong, S. Fourmaux, T. E. Glover, P. A. Heimann, J. C. Kieffer, and R. W. Schoenlein, *Phys. Rev. Lett.* **95**, 067405 (2005).
- ¹⁰S. Fourmaux, L. Lecherbourg, M. Harmand, M. Servol, and J. C. Kieffer, *Rev. Sci. Instrum.* **78**, 113104 (2007).
- ¹¹C. Gahl, A. Azima, M. Beye, M. Deppe, K. Döbrich, U. Hasslinger, F. Hennies, A. Melnikov, M. Nagasono, A. Pietzsch, M. Wolf, W. Wurth, and A. Föhlisch, *Nat. Photonics* **2**, 165 (2008).
- ¹²M. Nagasono, E. Suljoti, A. Pietzsch, F. Hennies, M. Wellhöfer, J.-T. Hoefl, M. Martins, W. Wurth, R. Treusch, J. Feldhaus, J. R. Schneider, and A. Föhlisch, *Phys. Rev. A* **75**, 051406(R) (2007).
- ¹³C. Bostedt, H. N. Chapman, J. T. Costello, J. R. Crespo López-Urrutia, S. Düsterer, S. W. Epp, J. Feldhaus, A. Föhlisch, M. Meyer, T. Möller, R. Moshammere, M. Richter, K. Sokolowski-Tinten, A. Sorokin, K. Tiedtke, J. Ullrich, and W. Wurth, *Nucl. Instrum. Methods Phys. Res. A* **601**, 108 (2009).
- ¹⁴A. Föhlisch, M. Nagasono, M. Deppe, E. Suljoti, F. Hennies, A. Pietzsch, and W. Wurth, *Phys. Rev. A* **75**, 013411 (2007).
- ¹⁵M. Martins, M. Wellhofer, J. T. Hoefl, W. Wurth, J. Feldhaus, and R. Follath, *Rev. Sci. Instrum.* **77**, 115108 (2006).
- ¹⁶M. Wellhöfer, M. Martins, W. Wurth, A. A. Sorokin, and M. Richter, *J. Opt. A, Pure Appl. Opt.* **9**, 749 (2007).